

Aquifers productivity in the Pan-African context

ARETOUYAP ZAKARI^{1,*}, NOUAYOU ROBERT¹, NJANDJOCKNOUCK PHILIPPE¹ and ASFAHANI JAMAL²

¹Postgraduate School of Science, Technology and Geosciences, University of Yaounde I,
P.O. Box 812 Yaounde, Cameroon.

²Applied Geophysics Division, Head Atomic Energy Commission, P.O. Box 6091, Damascus, Syria.

*Corresponding author. e-mail: aretouyap@gmail.com

In this study, 50 Vertical Electrical Soundings (VES) were carried out in the region, including 14 near existing boreholes for comparison. Aquifer parameters of hydraulic conductivity and transmissivity were obtained by analyzing pumping test data from existing boreholes. An empirical relationship between hydraulic conductivity (K) obtained from pumping test and both resistivity and thickness of the Pan-African aquifer has been established for these boreholes in order to calculate the geophysical hydraulic conductivity. The geoelectrical interpretation shows that almost all aquifers are made of the fractured portion of the granitic bedrock located at a depth ranging between 7 and 84 m. The hydraulic conductivity varies between 0.012 and 1.677 m/day, the resistivity between 3 and 825 Ω m, the thickness between 1 and 101 m, the transmissivity between 0.46 and 46.02 m²/day, the product $K\sigma$ between 2.1×10^{-4} and 4.2×10^{-4} .

1. Introduction

Depending on weather conditions, and geological and geomorphological contexts of each region, the water sector poses more difficulties. These difficulties may arise in terms of flood (too much water), dryness (very little water) or pollution (poor quality water). All these problems have a common consequence: the shortage of good quality water for domestic, agro-pastoral and industrial needs. In some semi-arid climate contexts, surface water has shown its limits due to climate aversion and poor spatial distribution of populations (Arétouyap *et al.* 2014). This explains the importance of groundwater in such regions and the interest that is brought to its potential exploration. The exploitation of this resource must be carried out with extreme diligence to ensure a long-term use (Asfahani 2007). Efficient management of groundwater resources depends on the accuracy in the detection and location of aquifers and in predicting

their behaviour during the upcoming exploitation. Indeed, one of the general handicaps faced by the exploitation of new aquifers is the lack of information on their properties (permeability, transmissivity, etc.) due to the limitation of the number of pumping tests.

Geophysical methods such as Vertical Electrical Sounding (VES) technique can contribute significantly to the accuracy of the aquifer location and productivity, not only by developing its geometry but also by establishing a relationship between the hydrogeological and geo-electrical parameters. Indeed, since the late 1960s, many researchers, scientists, engineers and hydrologists have used the resistivity method to obtain useful information about the aquifers such as hydraulic conductivity, transmissivity, and flow. Some of these studies are summarized in table 1.

Asfahani (2012, 2013 and 2014) has recently proposed two other inexpensive alternative approaches based on the use of surficial VES technique to

Keywords. Aquifer depth; geoelectrical surveys; hydraulic conductivity; ordinary kriging; Pan-African context; pumping test.

Table 1. Summarized table of literature review.

Author	Salient features	Application country
Jones and Bufford (1951)	Relationship between permeability and formation factor	USA
Croft (1971)	Relationship between permeability and formation factor	USA
Vincenz (1968)	Relationship between resistivity and well productivity	Mexico
Ungemach et al. (1969)	Relationship between transmissivity and transverse resistance	India
Scarascia (1976)	Assessment of the transmissivity through interpreting the electrical soundings	Italy
Kelly (1977)	Correlation between saturated thickness resistivities and hydraulic conductivities	England
Mazáč and Landa (1979)	Relationship between aquifer transmissivity and transverse resistance	Poland
Athavale et al. (1992)	Measurement of natural recharge	India
Frohlich et al. (1996)	Electrical hydraulic conductivity correlation in fractured crystalline bedrock	USA
Huntley (1986)	Relations between permeability and electrical resistivity in granular aquifers	India
Emenike (2001)	Groundwater exploration in a sedimentary environment	Nigeria
Yang and Lee (2002)	Hydrogeological studies	Taiwan
Chandra et al. (2004)	Groundwater exploration in hard rock areas	India
Asfahani (2007)	Determination of the characteristics of the Neogene aquifer	Syria
Nejad (2009)	Study of the water potential	Iran
Anomohanran (2013)	Study of the water potential	Nigeria

compute the aquifer hydraulic conductivity. His alternative approaches have been successfully applied for characterizing the transmissivity of the Quaternary and Paleogene aquifers in the semi-arid Khanasser valley region, northern Syria.

The main objectives of this paper are, therefore, the following:

1. Detecting and locating the aquifers in the Pan-African region by applying electrical resistivity surveys.
2. Characterizing those aquifers in terms of hydraulic conductivity, transmissivity, depth, thickness and resistivity.
3. Building up thematic maps of those mentioned characteristics by using the geostatistical ordinary kriging method.

2. Materials and methods

2.1 Study area

This study is carried out in the Pan-African region of Adamawa, located in the heart of central Africa between 6°–8°N latitude and 11°–16°E longitude (figure 1). It extends over a length of about 410 km from west to east between Nigeria and the central African Republic, for a total area of 67,827 km². From March to October, the region receives an average rainfall of 1540 mm per year. The temperature is moderate with an annual average around 25°C (Arétouyap et al. 2014). On the hydrological level, the Adamawa region is called ‘the water tower of Cameroon’ because it feeds three of the four major watersheds of this country, namely the

lake Chad basin, the Niger basin in the north and the Sanaga Atlantic basin in the south.

The study area consists of two major geological domains:

- The former basement that includes highly metamorphosed formations (migmatitic, gneiss and mica), and intrusive bodies composed of granites;
- The covering formations that include: red lateritic soils, sedimentary (sandstones and conglomerates) and volcanic (basalt and trachyte) rocks.

This region is the stool of a Pan-African granite-gneissic basement, represented by granites, gneisses and Pan-African migmatites. Geological formations encountered are basalts, trachytes and trachyphonolites based mostly on concordant and discordant alkaline granites (Toteu et al. 2000). There are two major fractures slanted towards in two directions:

- The first oriented N30°E (most common) is that of the ‘Cameroon volcanic line’;
- The second oriented N70°E, is the ‘Adamawa line’ or ‘shear area of Adamawa’.

The soils of the region are lateritic and classified into two types (Segalen 1967; Toteu et al. 2004): red soils derived from ancient metamorphic rocks and red soils formed on old basalts.

2.2 VES acquisition and data processing

Fifty VES have been carried out in the study region (figure 2), by using Schlumberger array in order

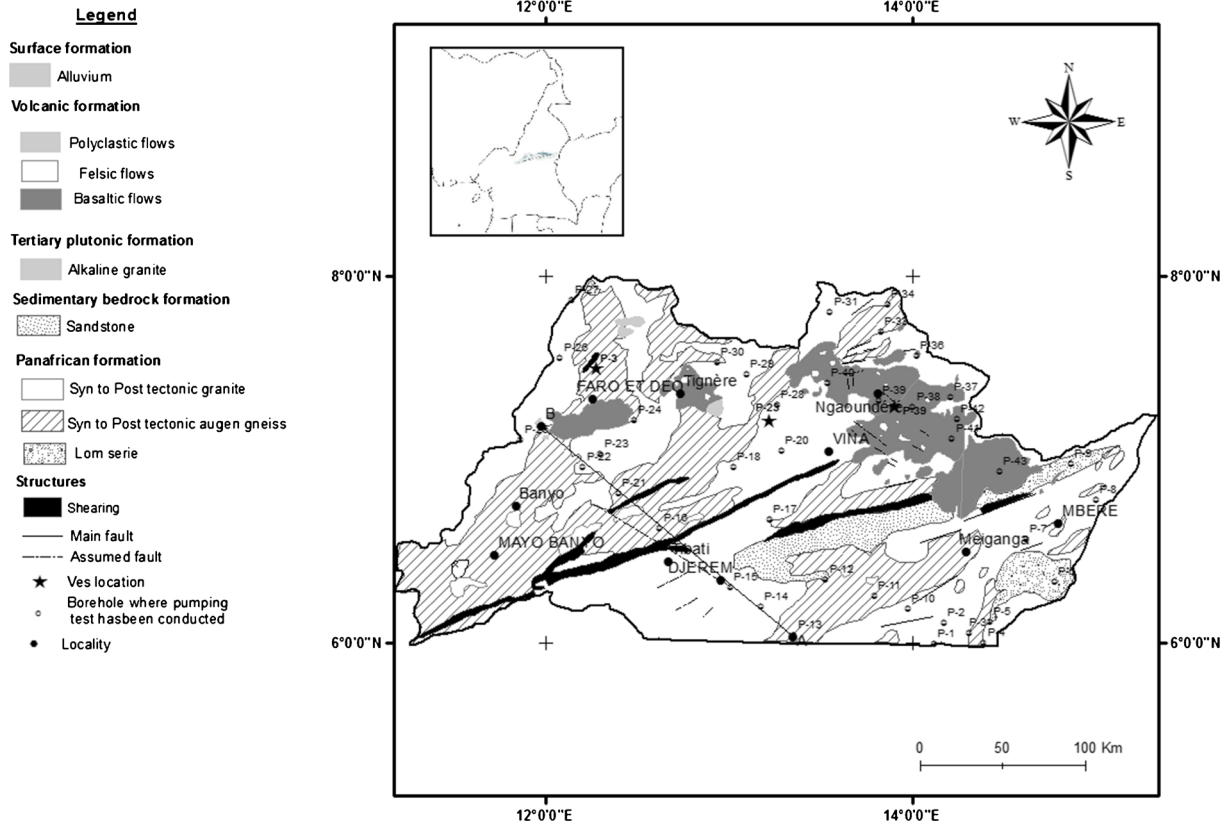


Figure 1. Simplified geological map of the study area.

to detect the aquifers and determine their electrical characteristics (Dar-Zarrouck parameters). ABEM terrameter (SAS 1000) was used to conduct those VES measurements, with current electrode separation (AB) varying from 1 to 300 m in successive steps. The SAS 1000 measures directly the resistance $\Delta V/I$, and apparent resistivity ρ_a is subsequently computed according to equation (1) (Dobrin 1976).

$$\rho_a = \frac{2\pi}{\left(\frac{1}{AM} - \frac{1}{BM} - \frac{1}{AN} + \frac{1}{BN}\right)} \frac{\Delta V}{I}, \quad (1)$$

where I is the current introduced into the earth by current electrodes, A and B , and ΔV are the potentials measured between the potential electrodes M and N .

The apparent resistivity values ρ_a obtained by increasing the electrode spacing around a fixed point are plotted against half electrode separation $AB/2$ in order to establish the field resistivity curve.

Interpretation of field resistivity curves is made by a curve matching technique using master curves (Asfahani 2011) for the initial determination of thicknesses and resistivities of corresponding layers (initial approximate model). The parameters of

this approximate model were accurately interpreted using an inverse technique program, until a goodness-of-fit between the field resistivity curve and the theoretical regenerated curve was obtained (Zohdy 1989; Zohdy and Bisdorf 1989). The quantitative interpretation of VES data has been made by adapting two main hypotheses as follows (Anomohanran 2013):

- the earth is horizontal, with the last layer being of infinite thickness;
- each layer is electrically homogeneous and isotopic.

The ordinary kriging technique is used to interpolate the hydrogeophysical investigation results in the overall region, even in the locations where VES measurements were not conducted. This kriging method involves three steps (Gorai and Kumar 2013):

1. Exploratory data analysis: the main role of this step is to check data consistency, remove outliers and identify statistical distribution where data came from, because kriging methods work best for normal distribution data. Normal data distribution is decided when the mean and the median are very similar. However, high skewness

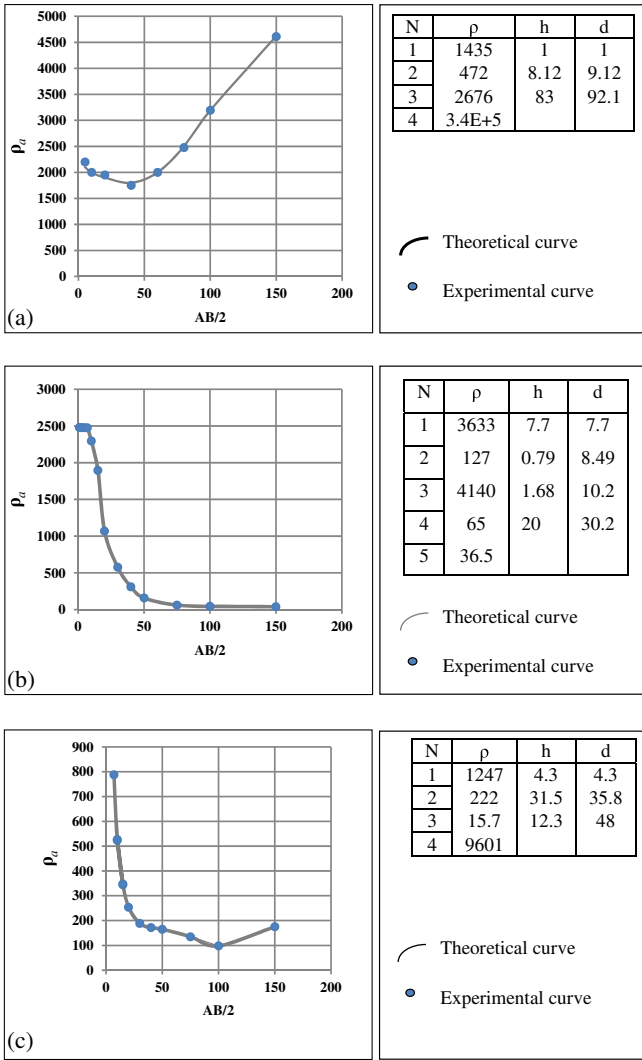


Figure 2. Examples of resistivity sounding curves with their interpretative models, measured on points of existing boreholes. (a) Resistivity curve measured at Beka-Mangari (P-3). (b) Resistivity curve measured at Kona Gaouri (P-23). (c) Resistivity curve measured at Nyambaka (P-39).

values indicate the existence of outliers, which are very high or low measured values compared to the dataset. The outliers are caused by a bad measurement or a bad recording, and must be transformed when they exist.

2. Structural data analysis: spatial correlation or dependence in the dataset will be quantified by using variograms. Kriging relates the variogram, the half expected squared difference between paired data values $z(x)$ and $z(x + h)$ to the distance lag h , by which locations are separated (equation 2).

$$\gamma(h) = \frac{1}{2}E [z(x) - z(x + h)]^2. \quad (2)$$

For discrete variables, this function can be written as shown in equation (3).

$$\gamma(h) = \frac{1}{2N(h)} \sum_{i=1}^{N(h)} [z(x_i) - z(x_i + h)]^2 \quad (3)$$

where $z(x_i)$ is the value of the variable Z at location x_i , h the lag, and $N(h)$ the number of pairs of VES locations separated by h . For irregular data, it is rare for the distance between the location pairs to be exactly equal to h . A variogram plot is obtained by calculating values of the variogram at different lags. These values are thereafter fitted with a theoretical model. The models provide information about the spatial structure as well as the input parameters for the kriging interpolation.

3. Prediction: seven variogram models (exponential, spherical, Gaussian, magnetic, gravimetric, pentaspherical and quadratic) were tested for each studied parameter (depth, thickness, hydraulic conductivity, and transmissivity of the aquifer) in order to select the best-fitted one. Predictive performances of the fitted models are checked on the basis of cross validation tests. The values of mean error (ME), mean square error (MSE), root mean square error (RMSE), average standard error (ASE), and root mean square standardized error (RMSSE) are estimated to ascertain the performance of the developed models. If the predictions are unbiased, the ME should be almost nil. But because of its weaknesses due to its dependence upon the scale of the data and to its indifference to the wrongness of variogram, ME is generally standardized by the MSE, being ideally zero.

However, RMSE and ASE should be calculated to indicate if the prediction errors were correctly assessed in the case where they are close. Otherwise, if the RMSE is less than the ASE (or RMSSE < 1), then the variability of the predictions is overestimated; and if the RMSE is greater than the ASE (or RMSSE > 1), then the variability of the predictions is underestimated. Once the best model is selected, it is used to draw the thematic map that provides the spatial distribution of the parameter to be estimated. All these errors are expressed by equations (4–8) below (Goovaerts 1997; Gorai and Kumar 2013).

$$ME = \frac{1}{N} \sum_{i=1}^N [Z^*(x_i) - Z(x_i)] \quad (4)$$

$$MSE = \frac{1}{N} \sum_{i=1}^N \left[\frac{Z^*(x_i) - Z(x_i)}{\sigma^2(x_i)} \right] \quad (5)$$

Table 2. Geoelectrical data interpretation results in the study area.

VES station	Layer resistivity (Ωm)					Layer thickness (m)				Layer conductance (Ω^{-1})				Layer resistance (Ωm^2)			
	ρ_1	ρ_2	ρ_3	ρ_4	ρ_5	h_1	h_2	h_3	h_4	σ_1	σ_2	σ_3	σ_4	R_1	R_2	R_3	R_4
P-1	8715	15905	811	1640	1529	2	3	4	25	0.0002	0.0002	0.0049	0.0152	17430	47715	3244	41000
P-2	6353	3621	4715	-	-	1	41	-	-	0.0002	0.0113	-	-	6353	148461	-	-
P-3	1435	472	2676	341250	-	1	8	83	-	0.0007	0.0172	0.0310	-	1435	307090	222108	-
P-4	11471	1757	120000	-	-	1	48	-	-	0.0001	0.0273	-	-	11471	84336	-	-
P-5	186	308	5	8705	-	5	20	6	-	0.0263	0.0649	1.2000	-	930	6160	30	-
P-6	2579	27383	157	4158	22	2	3	6	18	0.0008	0.0001	0.0382	0.0043	5158	82149	942	74844
P-7	444	444	137	2500	231	14	58	1	-	0.0315	0.1306	0.0073	-	6216	25752	137	-
P-8	591	134	2	793	-	11	43	5	-	0.0186	0.3209	2.5000	-	6501	5762	10	-
P-9	1377	345	207	12	2642	3	14	19	22	0.0022	0.0406	0.0918	1.8333	4131	4830	3933	264
P-10	10233	1141	28810	-	-	2	9	19	-	0.0002	0.0079	0.0007	-	20466	10269	547390	-
P-11	15845	4100	140000	-	-	4	40	-	-	0.0003	0.0098	-	-	63380	164000	-	-
P-12	1020	22	8654	-	-	9	37	-	-	0.0088	1.6818	-	-	9180	814	-	-
P-13	656	144	212	177	271	4	10	8	40	0.0061	0.0694	0.0377	0.2260	2624	1440	1696	7080
P-14	384	525	718	11256	-	12	8	130	-	0.0312	0.0152	0.1811	-	4608	4200	93340	-
P-15	1131	246	1129	355	-	12	15	17	-	0.0106	0.0610	0.0151	-	13572	3690	19193	-
P-16	510	2	211	46	-	21	4	46	-	0.0412	2.0000	0.2180	-	10710	8	9706	-
P-17	4865	7829	446	2800	-	5	24	31	-	0.0010	0.0031	0.0695	-	24325	187896	13826	-
P-18	15422	13369	408	3626	-	4	13	43	-	0.0003	0.0010	0.1054	-	61688	173797	17544	-
P-19	1308	613	26	4964	-	18	17	34	-	0.0138	0.0277	1.3077	-	23544	10421	884	-
P-20	3770	188	94	-	-	6	61	-	-	0.0016	0.3245	-	-	22620	11468	-	-
P-21	1683	6415	3926	3102050	-	1	9	70	-	0.0006	0.0014	0.0178	-	1683	57735	274820	-
P-22	8839	3328	341	152420	-	3	29	23	-	0.0003	0.0087	0.0674	-	26517	96512	7843	-
P-23	3633	127	4140	65	37	8	1	2	20	0.0022	0.0079	0.0005	0.3077	29064	127	8280	105820
P-24	15	502	11	2531	-	4	6	5	-	0.2667	0.0120	0.4545	-	60	3012	55	-
P-25	20133	6937	100	20245	-	8	17	22	-	0.0004	0.0025	0.2200	-	161064	117929	2200	-
P-26	8899	1526	1108	450000	-	2	8	38	-	0.0002	0.0052	0.0343	-	17798	12208	42104	-
P-27	6928	943	62	5	-	3	10	101	-	0.0004	0.0106	1.6290	-	20784	9430	6262	-
P-28	21	2215	8	-	-	11	19	-	-	0.5238	0.0086	-	-	231	42085	-	-
P-29	413	522	13	653	28	3	3	6	48	0.0073	0.0057	0.4615	0.0735	1239	1566	78	31344
P-30	3386	544	825	200	-	4	9	38	-	0.0012	0.0165	0.0461	-	13544	4896	31350	-
P-31	25464	9834	565	150000	-	10	18	40	-	0.0004	0.0018	0.0708	-	254640	177012	22600	-
P-32	988	25	3885	-	-	17	33	-	-	0.0172	1.3200	-	-	16796	825	-	-
P-33	739	25	479	33	-	17	11	42	-	0.0230	0.4400	0.0877	-	12563	275	20118	-
P-34	419	4003	10	66	-	2	5	11	-	0.0048	0.0012	1.1000	-	838	20015	110	-
P-35	1900	1179	387	58	-	5	9	14	-	0.0026	0.0076	0.0361	-	9500	10611	5418	-

Table 2. (Continued.)

VES station	Layer resistivity (Ωm)					Layer thickness (m)				Layer conductance (Ω^{-1})			Layer resistance (Ω^2)				
	ρ_1	ρ_2	ρ_3	ρ_4	ρ_5	h_1	h_2	h_3	h_4	σ_1	σ_2	σ_3	σ_4	R_1	R_2	R_3	R_4
P-36	210	53	9699	-	-	4	62	-	-	0.0190	1.1699	-	-	840	3290	-	-
P-37	15677	7840	422	170000	-	4	24	28	-	0.0003	0.0031	0.0664	-	62708	188160	11816	-
P-38	853	4	1872	-	-	18	21	-	-	0.0211	5.2500	-	-	15354	84	-	-
P-39	1247	222	16	9601	-	4	32	12	-	0.0032	0.1441	0.75	-	4988	7104	355466	-
P-40	4597	333	40	14126	-	3	25	61	-	0.0007	0.0751	1.5250	-	13791	8325	2440	-
P-41	1336	1300	200	44172	-	2	10	38	-	0.0015	0.0078	0.1900	-	2672	13000	7600	-
P-42	748	3	104	5217	-	16	17	33	-	0.0214	5.6667	0.3173	-	11968	51	3432	-
P-43	3198	255	2120	20	-	4	14	52	-	0.0013	0.0549	0.0245	-	12792	3570	110240	-
P-44	2003	61	4134	-	-	6	93	-	-	0.0030	1.5246	-	-	12018	5673	-	-
P-45	771	3	2879	-	-	26	8	-	-	0.0337	2.6667	-	-	20046	24	-	-
P-46	38	20	239	-	-	7	7	-	-	0.1842	0.3500	-	-	266	140	-	-
P-47	95	11	2161	11	-	20	8	15	-	0.2105	0.7273	0.0069	-	1900	88	32415	-
P-48	147	7	640	7	-	7	5	30	-	0.0476	0.7143	0.0469	-	1029	35	19200	-
P-49	11254	2016	2704	6	-	8	14	32	-	0.0007	0.0069	0.0118	-	90032	28224	86528	-
P-50	989	47	5270	-	-	17	85	-	-	0.0172	1.8085	-	-	16813	3995	-	-

$$RMSE = \sqrt{\frac{1}{N} \sum_{i=1}^N [Z^*(x_i) - Z(x_i)]^2} \quad (6)$$

$$ASE = \sqrt{\frac{1}{N} \sum_{i=1}^N \sigma^2(x_i)} \quad (7)$$

$$RMSSE = \sqrt{\frac{1}{N} \sum_{i=1}^N \left[\frac{Z^*(x_i) - Z(x_i)}{\sigma^2(x_i)} \right]^2} \quad (8)$$

where $\sigma^2(x_i)$ is the kriging variance for location x_i , $Z^*(x_i)$ and $Z(x_i)$ are the estimated and the measured values of the parameter at the location x_i , respectively.

2.3 The hydrogeophysical model parameters

The hydraulic conductivity (K) of an aquifer is the main hydrogeological property for the overall region. It refers to the ability of the aquifer to receive the infiltrated water, and expressed in m/day. Fourteen available boreholes exist in the study region (figure 1), where traditional pumping tests have been conducted, and enabled to evaluate the hydraulic conductivity values on those boreholes.

This paper applies the technique already developed by Asfahani (2007). This technique consists of the following steps:

1. Plotting a calibration line of the empirical relationship between the transverse resistance R of the aquifer obtained by VES interpretations, carried out in the 14 VES locations near the boreholes, and $K\sigma$, where K is the hydraulic conductivity parameters obtained by pumping tests from the 14 available boreholes in the study area.
2. Determining the Dar-Zarrouck parameters (transverse resistance R and longitudinal conductance S) given by equations (9) and (10) for the other 36 VES points, where no borehole exists.

$$R = \sum_{i=1}^n h_i \rho_i \quad (9)$$

$$S = \sum_{i=1}^n \frac{h_i}{\rho_i} \quad (10)$$

where h_i and ρ_i are the thickness and the resistivity of i th layer in the section, respectively.

The transmissivity at each VES location is deduced by equation (11), by taking into consideration the transmissivity and the transverse

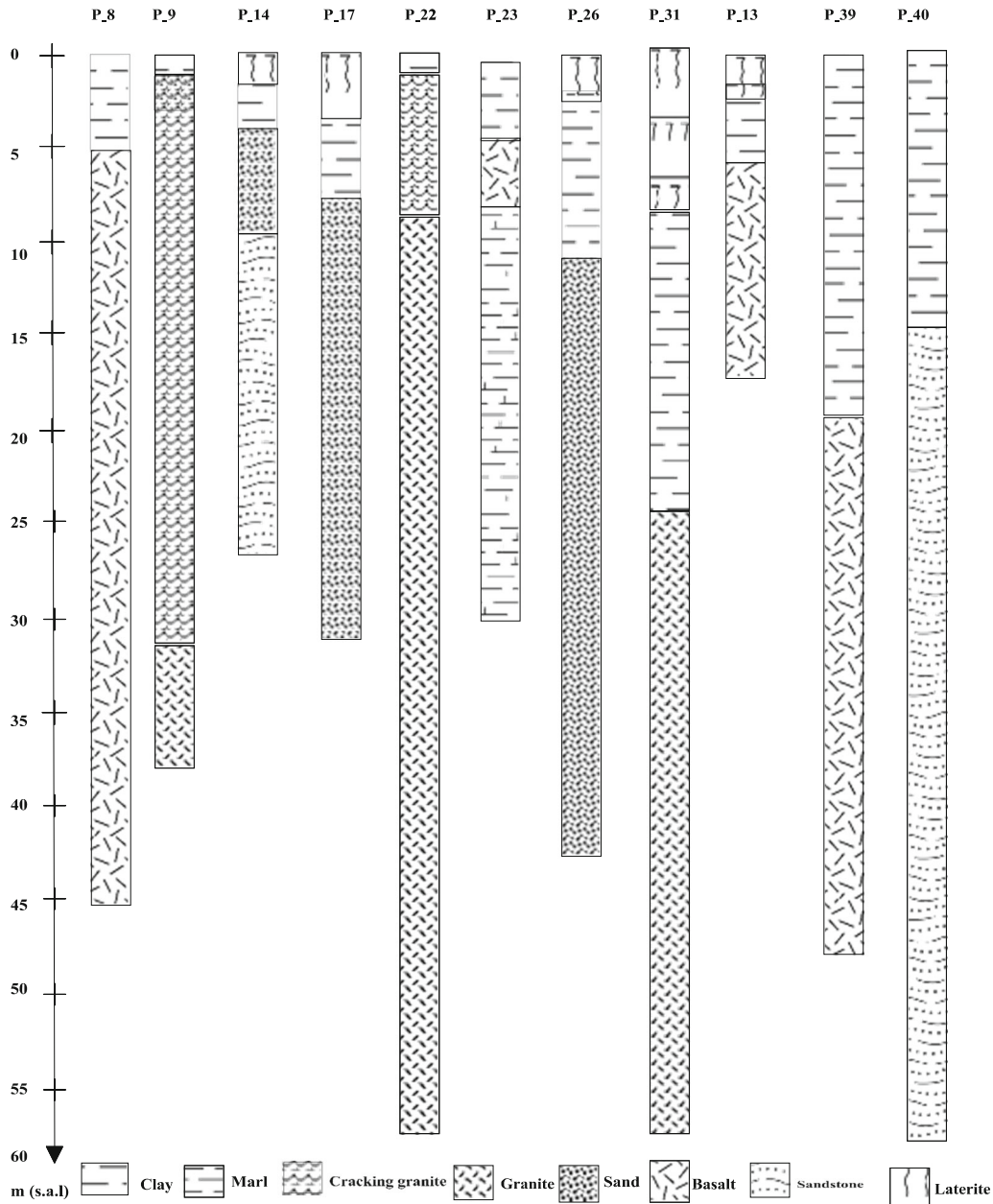


Figure 3. Lithological sections of 11 boreholes logged to highlight the vertical variation of the lithology.

conductance for each layer (equations 12 and 13).

$$T = K\sigma R = Kh \tag{11}$$

where K is the hydraulic conductivity of the aquifer, σ its electric conductivity, R its transverse resistance and h its depth.

$$S_i = \sigma_i h_i \tag{12}$$

where σ_i is the layer conductivity.

$$Tr_i = K_i h_i \tag{13}$$

where K_i is the hydraulic conductivity of the i th layer with thickness h_i .

3. Using the empirical relationship explained in step 1 to compute $K\sigma$ and, consequently, K for each VES location.

3. Results and discussion

Fifty VES with Schlumberger configuration have been carried out in the study area and interpreted. Figure 2 shows the resistivity curves obtained at 3 of the 14 existing boreholes (P-3, P-23, and P-39) and their interpretative models, and a summary of the results for all the sounding stations is presented in table 2. The VES interpreted results have been mainly calibrated through referring to the

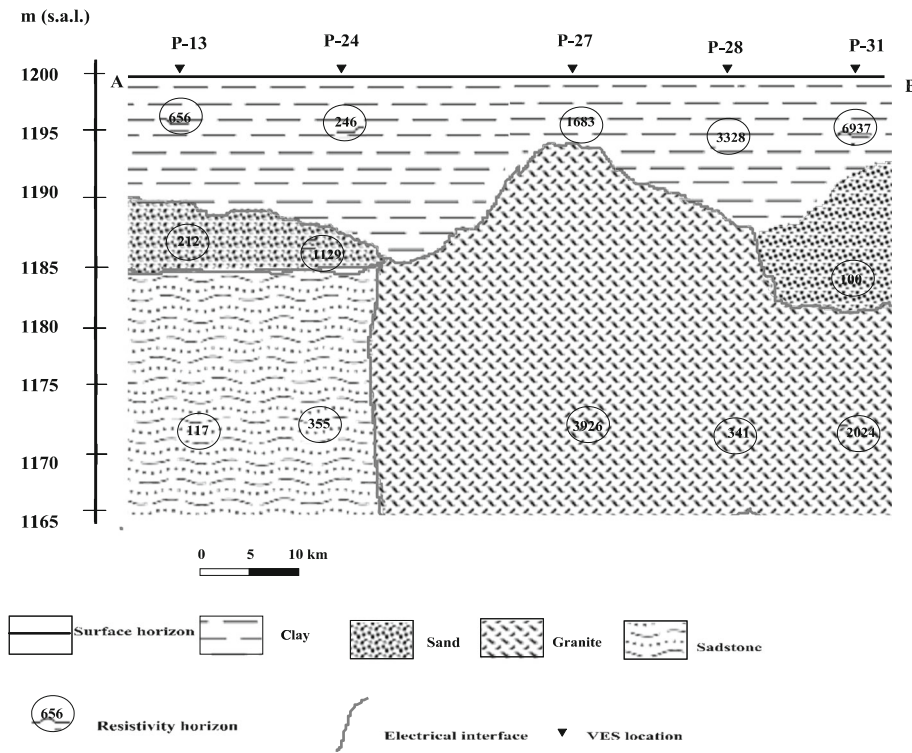


Figure 4. Lithological cross-section along the profile A-B.

geolectrical response acquired from surface outcrops of different formations and to the lithological information obtained from eleven boreholes logged on the locations of P-8, P-9, P-14, P-17, P-22, P-23, P-26, P-31, P-33, P-39 and P-40 (figure 3).

The quantitative interpretation allows the construction of the lithological cross-section along the profile A-B that matches stations P-24, P-27, P-28 and P-31 in southeast-northwest direction (figure 4).

This interpretation is used to detect and locate the aquifers and to determine the lithology of each VES location. The application of the approach developed by Asfahani (2007) enables to establish an empirical relationship between $K\sigma$ and R from the 14 boreholes existing in the region (equation 14) as shown in figure 5.

$$K\sigma = -10^{-14}R + 5.10^{-9}. \quad (14)$$

The application of equation (14) enables to compute the $K\sigma$ in all the VES locations and consequently derive the hydraulic conductivity K in each VES location.

The study of the profile A-B indicates the existence of two types of geological array:

1. The first type is located at the middle of the profile and has three geological horizons. The first horizon is laterite or topsoil with a thickness varying between 0.5 and 1.5 m. Laterite generally has a high resistivity up to 4000 Ωm .

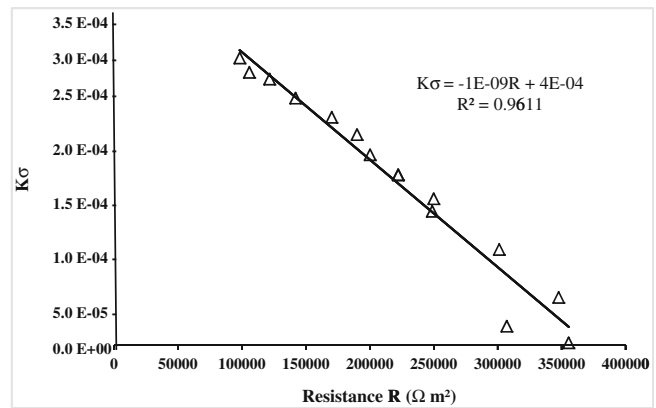


Figure 5. Calibration line of the empirical relation between R and $K\sigma$.

The second horizon is a clayey soil. Its thickness varies from 5 to 15 m, and its resistivity ranges between 200 and 7000 Ωm . The third horizon is the granitic bedrock. Its upper part represents the aquifer when it is altered or cracked. Its thickness varies between 1 and 101 m, and depending on the degree of the alteration, its resistivity varies between 3 and 825 Ωm . When this horizon is not fractured, it is impermeable and constitutes the Pan-African base. In this case, its resistivity can reach thousands of ohm-meters.

2. The second type of geological array is observed at the ends of the profile and has four geological

horizons. The first and the second horizons remain laterite/topsoil and clayey soil with the same proprieties, respectively. The third horizon is a sandy soil. Its thickness varies from 1 to 15 m, and its resistivity ranges between 100 and 1300 Ω m. In the southwest region, the fourth horizon representing the aquifer is composed of sandstone. Its thickness varies between 20 and 61 m, and its resistivity varies between 47 and 355 Ω m.

In general, the Pan-African aquifer in the study area is made of cracked upper part of granite or sandstone. This is the third or the fourth geoelectrical horizon.

The thickness of this Pan-African aquifer varies between 1 and 101 m, with an average of 34.16 m and a standard deviation (SD) of 22.67 m. Its resistivity varies between 3 and 825 Ω m with an average of 228.48 Ω m and an SD of 215.87 Ω m. Figures 6 and 7 show the maps of resistivity and thickness variation of this Pan-African aquifer in the study area, respectively. The resistivity map indicates the presence of a low-resistivity zone, reflecting the potential direction of groundwater from north to south, and from northeast (where the recharge area is located) to southeast.

Table 3 indicates the properties of the aquifer at the 3 of 14 points (Beka-Mangari, Kona-Gaouri, and Nyambaka) where pumping tests were carried

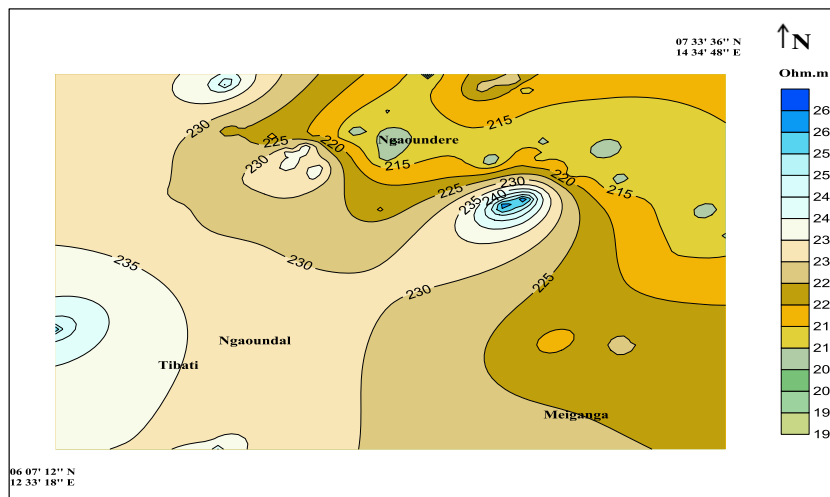


Figure 6. Thematic map of the aquifer resistivity.

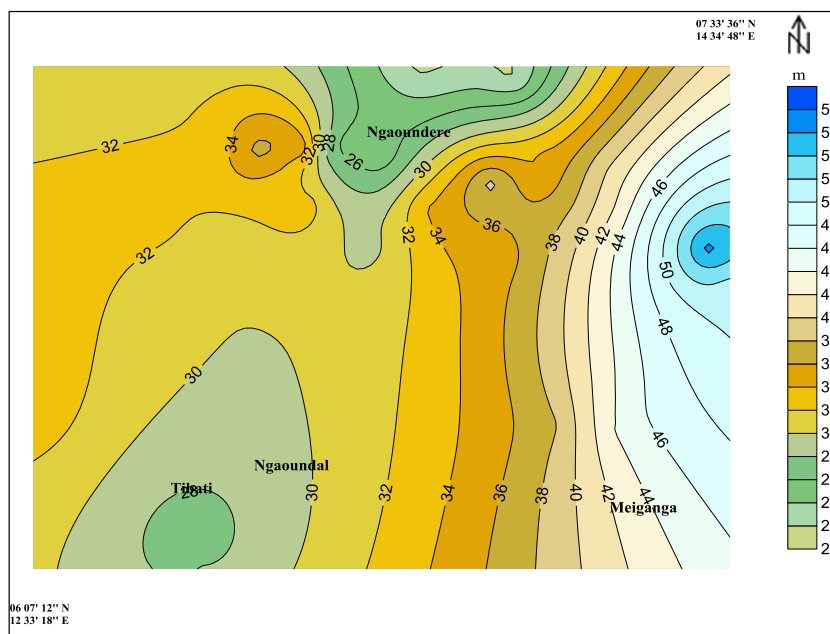


Figure 7. Thematic map of the aquifer thickness.

Table 3. *Aquifer properties of three existing boreholes in the study area.*

Parameter	Beka-Mangari (P-3)	Kona Gaouri (P-23)	Nyambaka (P-39)
1 Hydraulic conductivity K (m·day ⁻¹) obtained from pumping test	0.15	0.79	0.21
2 Aquifer resistivity ρ (Ω m)	472	48	28
3 Aquifer thickness h (m)	8.4	16.2	11.8
4 Longitudinal conductance S (Ω^{-1})	0.017324	0.3375	0.421
5 Transverse resistance R (Ω m ²)	307090	105820	355466
6 K/σ ($\times 10^3$)	1.11	2.21	0.163
7 $K\sigma$ ($\times 10^{-5}$)	2.00	0.285	26
8 Aquifer transmissivity T_{ri} (m ² ·day ⁻¹)	1.2489	12.861	2.4214
9 Hydraulic conductivity K (m·day ⁻¹) derived from VES measurements	0.148	0.779	0.205

Table 4. *Characteristics of the Pan-African aquifer in the study area.*

	h (m)	ρ (Ω m)	T_{ri} (m ² /day)	K (m/day)	S (Ω^{-1})	$K\sigma$ ($\times 10^{-4}$)
Min	1	3	0.46	0.012	0.004	1.46
Max	101	825	46.02	1.677	5.25	428.54
Average	34.16	228.48	15.46	0.456	0.61	28.49
SD	22.67	215.87	10.33	0.400	0.9	99.04

out. The values of the resistivity of the aquifer vary hugely 28 (P-39) to 472 Ω m (P-3). This is mainly explained by the nature of the aquifer studied. Indeed, contrary to sedimentary aquifers that are generally continuous, base aquifers are rather discontinuous and the value of their resistivity depends mainly on the degree of the bedrock fracturing or alteration. The granitic bedrock is then more fractured in Nyambaka (P-39) than Beka-Mangari (P-3).

Exact agreement for these three borehole locations is noted between the hydraulic conductivity derived from the geoelectrical data interpretation (parameter 9) and that obtained by pumping tests (parameter 1), as shown in table 4. Parameter 8 indicates the computed transmissivity of the aquifer by means of the geoelectrical parameters mentioned previously. Therefore, knowing the hydraulic conductivity from the pumping tests from the existing boreholes and R (or S) from the geoelectrical data interpretation, the transmissivity T_r and its variation from one place to another (including areas where borehole data are not available) have been evaluated through establishing an empirical relationship between those parameters, as explained previously. The transmissivity values determined from geoelectrical measurements according to equation (11) and shown in figure 8 are generally low over the entire area due to the known water scarcity in the study area. The transmissivity values vary between 0.46 and 46.02 m²·day⁻¹, with an average of 15.46 m²·day⁻¹ and an SD of 10.33 m²·day⁻¹. Comparison of figure 8 (transmissivity) with figure 7

(thickness of Pan-African aquifer) shows that areas underlain by relatively thick aquifer materials have higher transmissivity values than areas underlain by relatively thin aquifer materials. This relationship is expected, because transmissivity is a linear function of aquifer thickness, since hydraulic conductivity is assumed to be constant (Asfahani 2007).

Table 3 shows that aquifer resistivity which is higher in Beka-Mangari is the highest contrary to the transmissivity that is the lowest. Certainly, transmissivity is a linear function of resistivity according to equations (9 and 11). But it also depends on the aquifer thickness and hydraulic. This can also be explained by the geological composition of the soil.

Figure 9 shows the hydraulic conductivity map of the study area, where the values of this parameter range between 0.012 and 1.677 m·day⁻¹, with an average of 0.456 m·day⁻¹ and an SD of 0.400 m·day⁻¹.

According to the product of $K\sigma$, the study area has two main trends as shown in figure 10: a low- $K\sigma$ value zone in the centre and a high-value zone around the study area. The product of $K\sigma$ varies very slightly in the study area. It ranges from 2.1×10^{-4} to 4.2×10^{-4} , with an average of 3.47×10^{-4} and an SD of 0.84×10^{-4} . In light of the different geoelectrical results gathered, the characteristics of the Pan-African aquifer in the study area are summarized in table 4.

The aquifer depth varies generally from 14 to 70 m with most localities around 34 m (figure 11). Given the accessibility of aquifers (no huge depths), the

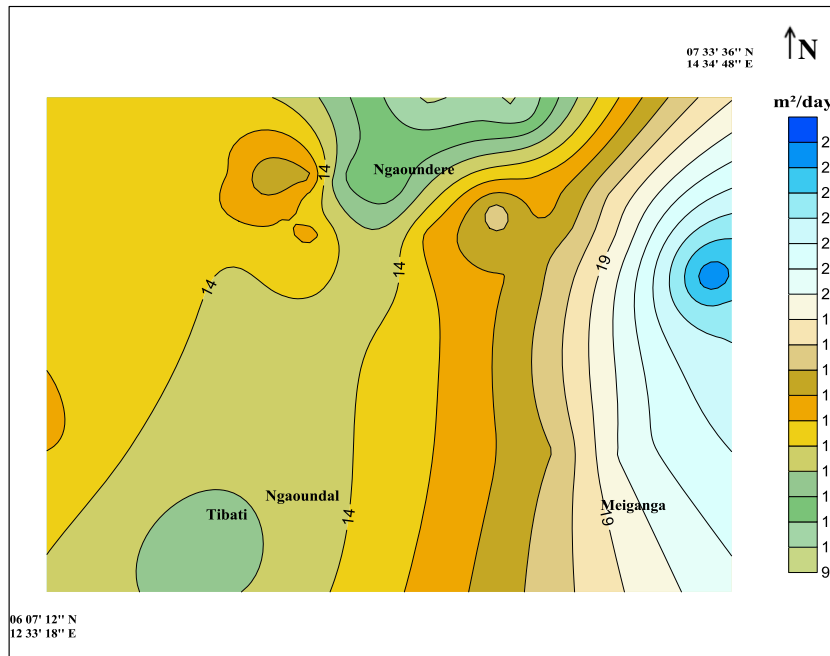


Figure 8. Thematic map of transmissivity.

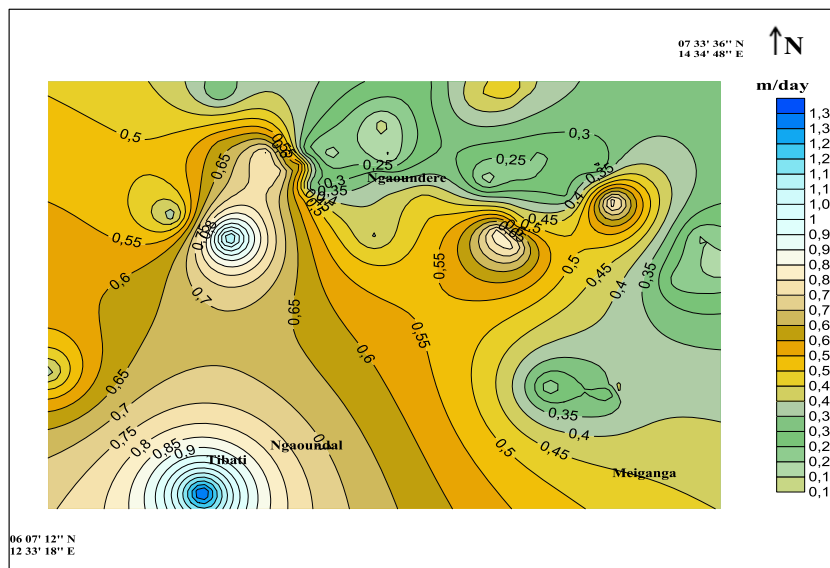


Figure 9. Thematic map of hydraulic conductivity.

main criteria for siting a borehole or a well are the hydraulic conductivity (for the ability to recharge) and physicochemical properties (for potability). The second criterion will be investigated during imminent studies while figure 10 shows that the northern part of the study area is more conductive and better rechargeable.

The knowledge of the characteristics of the studied parameters in the study area is important for integration in a scientific methodology

oriented towards the optimum exploitation of the Pan-African aquifer.

The equation used to determine hydrodynamic parameters from Dar-Zarrouck electrical parameters is an empirical relationship. In order to increase its reliability, the study area should be divided into small areas according to their respective geological features. For this, the other experimental boreholes will be drilled in the region.

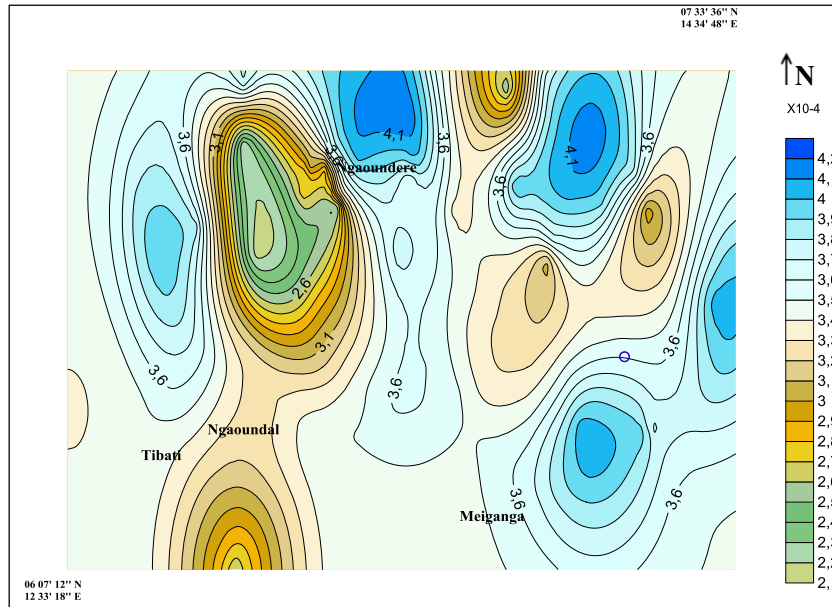


Figure 10. Thematic map of $K\sigma$.

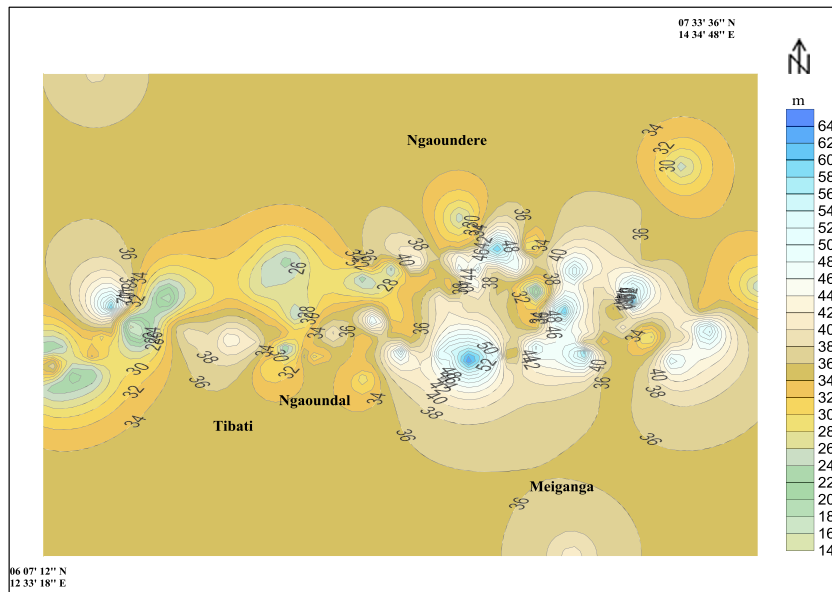


Figure 11. Thematic map of the depth where aquifer is situated.

4. Conclusions

Evaluation of hydraulic conductivity K from surface resistivity measurements is possible, through developing relationships between the electrical Dar-Zarrouk parameters of R or S and hydraulic conductivity from pumping tests on existing boreholes in the Pan-African context. This study reveals that Pan-African aquifers are characterized by a depth ranged between 7 and 83 m with an average of 37 m, a transverse conductance ranged from 0.004 to 5.25 Ω^{-1} with an average of 0.61 Ω^{-1} ,

a resistivity ranged from 3 to 825 Ωm with an average of 228 Ωm , a transmissivity ranged between 0.46 and 46.02 m^2/day and a hydraulic conductivity ranged from 0.012 to 1.677m/day with an average of 0.465m/day.

Acknowledgements

The first author would like to thank Dr Atangana Kouna Basile, Cameroonian Minister of Water Resources and Energy, for the permission to access

to the archives and records of all his national and regional services.

References

- Anomohanran O 2013 Geophysical investigation of groundwater potential in Ukelegbe, Nigeria; *J. Appl. Sci.* **13** 119–125.
- Arétouyap Z, Njandjock Nouck P, Bisso D, Nouyou R, Lengué B and Lepatio Tchieg A 2014 Climate variability and its possible interactions with water resources in central Africa; *J. Appl. Sci.* **14**(19) 2219–2233.
- Asfahani J 2007 Neogene aquifer properties specified through the interpretation of electrical sounding data, Salamiyeh region, central Syria; *Hydrol. Process.* **21** 2934–2943.
- Asfahani J 2011 The role of geoelectrical DC methods in determining the subsurface tectonic features: Case studies from Syria; In: *Tectonics* (ed.) Damien Closson, *Tech. Europe: Rijeka*, pp. 275–302.
- Asfahani J 2012 Quaternary aquifer transmissivity in semi-arid region in Khanasser Valley, northern Syria; *Acta Geophys.* **60** 1143–1158.
- Asfahani J 2013 Groundwater potential estimation deduced from vertical electrical sounding measurements in the semi-arid Khanasser Valley region, Syria; *Hydrol. Sci. J.* **58** 468–482.
- Asfahani J 2014 Hydraulic conductivity estimation by using an approach based on vertical electrical soundings in the semi-arid Khanasser Valley Region, Syria, *Environ. Earth Sci.* (submitted).
- Athavale R N, Rangarajan R and Murlidharan D 1992 Measurement of natural recharge in India; *J. Geol. Soc. India* **39** 235–244.
- Chandra S, Ananda Rao V and Singh V S 2004 A combined approach of Schlumberger and axial pole-dipole configurations for groundwater exploration in hard rock areas; *Curr. Sci.* **86** 1437–1443.
- Croft M G 1971 A method of calculating permeability from electric logs; In: *US Geological Survey Staff, Geological Survey Research* 1971, Chapter B. US Geological Survey Professional Paper 750-B, US Geological Survey: B265–B269.
- Dobrin M B 1976 Introduction to geophysical prospecting (McGraw-Hill: New-York), 144p.
- Emenike E A 2001 Geophysical exploration for groundwater in a sedimentary environment: A case study from Nanka over Nanka formation in Anambra Basin south-eastern Nigeria; *Global J. Pure Appl. Sci.* **7** 254–262.
- Frohlich R K, Fisher J J and Summerly E 1996 Electrical hydraulic conductivity correlation in fractured crystalline bedrock: Central Landfil, Rhode Island, USA; *J. Appl. Geophys.* **35** 249–259.
- Goovaerts P 1997 Geostatistics for natural resources evaluation; Oxford University Press, Applied Geostatistics Series, 365p.
- Gorai A K and Kumar S 2013 Spatial distribution analysis of groundwater quality index using GIS: A case study of Ranchi Municipal Corporation (RMC) area; *Geoinfor. Geostat: An overview* **1**(2), <http://dx.doi.org/10.4172/2327-4581.1000105>.
- Huntley D 1986 Relation between permeability and electrical resistivity in granular aquifer; *Ground Water* **24** 466–475.
- Jones P H and Bufford T B 1951 Electric logging applied to groundwater exploration; *Geophysics* **1** 115–139.
- Kelly W E 1977 Geoelectric sounding for estimating aquifer hydraulic conductivity; *Ground Water* **15** 420–424.
- Mazáč O and Landa I 1979 On determination of hydraulic conductivity and transmissivity of granular aquifers by vertical electric sounding; *J. Geol. Sci.* **16** 123–139.
- Nejad 2009 Geoelectric investigation in the aquifer characteristics and groundwater potential in Behbahan Azad University farm, Khuzestan Province, Iran; *J. Appl. Sci.* **9** 3691–3698.
- Scarascia S 1976 Contributions of geophysical methods to the management of water resources; *Geoexploration* **14** 265–266.
- Segalen P 1967 Les sols et la géomorphologie du Cameroun; *Cahier ORSTOM-Série Pédologie* **5** 137–187.
- Toteu S F, Ngako V, Affaton P, Nnange J M and Njanko T H 2000 Pan-African tectonic evolution in central and southern Cameroon: Transpression and transtension during sinistral shear movements; *J. African Earth Sci.* **36** 207–214.
- Toteu S F, Penaye J and Poudjom Djomani Y 2004 Geodynamic evolution of the Pan-African belt in central Africa with special reference to Cameroon; *Can. J. Earth Sci.* **41** 73–85.
- Ungemach P, Mostaghimi F and Dupart A 1969 Essais de détermination du coefficient d'emmagasinement en nappe libre, application à la nappe alluviale du Rhin; *Bulletin de l'Association Internationale d'Hydrologie Scientifique* **14** 169–190.
- Vincenz S A 1968 Resistivity investigations of limestone aquifers in Jamaica; *Geophysics* **33** 980–994.
- Yang C and Lee V 2002 Using direct current resistivity sounding and geostatistics to aid in hydrogeological studies in the Choshuichi Alluvial Fan, Taiwan; *Ground Water* **40** 165–173.
- Zohdy A A R 1989 A new method for the automatic interpretation of Schlumberger and Wenner sounding curves; *Geophysics* **54** 245–253.
- Zohdy A A R and Bisdorf R J 1989 Schlumberger sounding data processing and interpretation program; US Geological Survey, Denver, 74p.